Supporting Information for

Structure of a ferryl mimic in the archetypal iron(II)- and 2-(oxo)-glutarate-dependent dioxygenase, TauD

Katherine M. Davis[a], Madison Altmyer[b], Ryan J. Martinie[a], Irene Schaperdoth[a], Carsten Krebs[a,b], J. Martin Bollinger, Jr.[a,b], Amie K. Boal[a,b,*]

[a]Department of Chemistry and [b]Department of Biochemistry and Molecular Biology, The Pennsylvania State University, University Park, PA 16802, United States

Table of Contents

Experimental Methods

Growth, Expression and Purification of TauD

Cells were grown and TauD was purified as described in Price *et al.* with minor modifications.[1] The TauD gene, cloned into a pET22b vector, was overexpressed in BL21(DE3) *E. coli* cells (both Novagen, Madison WI). Cells were grown shaking at 37 °C in enriched medium (35 g/l tryptone, 20 g/l yeast extract, 5 g/l NaCl, at pH 7.3 with 150 mg/l ampicillin) to an OD_{600} of 0.8-1.0. After cooling for 30 min on ice, and induction of protein overexpression by addition of 0.2 mM IPTG (final concentration), cells were incubated shaking at 18 °C for an additional 18h. Cells were harvested by centrifugation (7000*g*, 20 min, 4 °C), flash frozen in liquid nitrogen and stored at -80°C.

All purification steps were carried out at 4 °C. In a representative preparation, 100 g of cells were resuspended in 500 mL buffer A [50 mM Tris-HCl, pH 7.6, 10 % (v/v) glycerol], and 44 mg/L phenyl methyl sulfonyl fluoride (PMSF, Amresco). The cells were lysed using a microfluidizer (Microfluidics M-110EH-30) and debris pelleted at 20,000 *g* for 20 min with subsequent clarification via a 0.17% polyethylene imine filter (PEI, Sigma). After centrifugation at 16,000*g* for 10 min, the supernatant was brought to 60% saturation (w/v) by addition of ammonium sulfate. Proteins were precipitated at 22,000*g* for 13 min. The pellet was redissolved in buffer A supplemented 1 mM EDTA and 1 mM DTT. The protein solution was dialyzed twice against 4 L of the same buffer to remove residual ammonium sulfate and other salts/metal ions.

The TauD protein was additionally purified using a DEAE Sepharose FF column equilibrated in buffer A, and eluted with a linear gradient of 0.05 – 0.2 M NaCl in buffer A. Fractions were analyzed for purity using SDS-PAGE. The fractions containing >95% TauD were concentrated with a Macrosep Advance centrifugal device, 10 kDa MWCO (Pall Corporation). The protein was dialyzed twice against 4 L of buffer A. TauD fractions were then applied to a MonoQ column (GE Healthcare, bed volume 1.7 ml) in several injections, each < 30 mg total protein. The column was washed with buffer A and proteins were eluted in a linear gradient of 0 – 0.2 M NaCl in buffer A. Fractions were analyzed by SDS-PAGE electrophoresis and those containing TauD were pooled and concentrated as described above. In a final purification step, the protein solution was loaded onto a Superdex 200 size exclusion column with isocratic elution in buffer A supplemented with 0.2 M NaCl. After exchange into buffer A lacking salt, pooled fractions were concentrated to 34.5 mg/mL for crystallization experiments.

Crystallization

Crystallization of TauD was performed in an anoxic glove box (Coy Laboratory Products) containing an atmosphere of approximately 97% N_2 and 3% H_2. All solutions were rendered O_2-free prior to use. To generate the TauD•(V^{IV}-oxo)•taurine•succinate complex in solution, a small volume of 50 mM vanadyl sulfate in 2.5 mM sulfuric acid was added to a stock solution of TauD at 34.5 mg/mL in 50 mM HEPES at pH 7.5. The solution was gently mixed and subsequently diluted with buffer, taurine and succinate to yield a final protein concentration of 21 mg/mL with 1.3 equivalents of vanadyl and 5 equivalents of substrate and co-product, respectively. The

resulting solution was incubated for a minimum of 5 min. at 4 °C before mixing in 1:1 proportion with a precipitant solution of 0.1 M Na acetate, pH 4.25, and 24% (w/v) PEG 300. Drops were allowed to equilibrate with a 500 μL reservoir of precipitant solution in a hanging drop vapor-diffusion experiment. Crystals appeared within 30 days and grew to size slowly over the following few months. Upon looping, thick rod-like crystals were soaked in a cryo-protectant generated by adding 27% (v/v) ethylene glycol to the reservoir condition before flash freezing in liquid nitrogen.

Data Collection and Processing

Diffraction data were collected on a MARmosaic 300 CCD detector at beamline 21-ID-G of the Advanced Photon Source at Argonne National Laboratory (Chicago, IL). The crystal was maintained at 100 K to minimize x-ray-induced damage while images were collected sequentially ($\Delta\phi = 1°$) at an incident wavelength of 0.97857 Å. Indexing, merging and scaling of the data was carried out in the HKL2000 software package.[2] The resolution of the dataset was subsequently cut at 1.75 Å for phasing, and molecular replacement was performed using the BALBES automatic molecular replacement pipeline.[3] A previously-solved structure of TauD with Fe(III), taurine and 2OG bound (PDB accession code 1GY9A)[4] was ultimately selected as the best search model. Model building and refinement were performed using Coot[5] and the Phenix software suite,[6] respectively. The obtained solution belongs to the $P2_12_12$ space group and contains two molecules in the asymmetric unit. Residues 3-283 were modeled in each chain. Metal-oxo restraints for vanadyl were initially defined by the geometry observed in the VioC•(V^{IV}-oxo)•L-Arg•succinate structure (PDB accession code 6ALR), but restraints were later relaxed, resulting in final V–O distances of 1.81 Å and 1.94 Å for chains A and B, respectively. Selected data processing and refinement statistics are presented in Table1.

Table S1. Crystallographic data processing and refinement statistics for TauD•(V^{IV}-oxo) •taurine•succinate structures.

PDB ID	6EDH
Data Collection[a]	
Space group	$P2_12_12$
Unit cell (Å)	a = 118.41, b = 54.20, c = 87.39 $\alpha = \beta = \gamma = 90$
Wavelength (Å)	0.97857
Resolution range (Å)	36.35 – 1.73 (1.79 – 1.73)
Total observations	775006 (77460)
Total unique observations	58939 (5830)
I/σ_I	23.27 (1.96)
Completeness (%)	99.0 (99.25)
R_{merge}	0.06711 (1.168)
R_{pim}	0.01894 (0.3252)
Redundancy	13.1 (13.3)
CC1/2	1 (0.834)
Refinement Statistics	
Resolution range (Å)	36.35 – 1.73
Reflections (total)	58910 (5829)
Reflections (test)	1712 (170)
Total atoms refined	4907
Solvent	307
R_{work} (R_{free})	17.46 (20.00)
rmsd	
Bond lengths (Å)/ angles (°)	0.003/0.67
Ramachandran plot	
Favored/allowed (%)	96.95/3.05
Mean B values (Å^2)	
Protein chains A/B	39.7/36.8
Vanadyl (A,B)/TAU/SIN/ACT	34.0,32.3/34.1/38.7/42.0
Solvent	41.68

[a] Values in parentheses refer to the high-resolution shell.

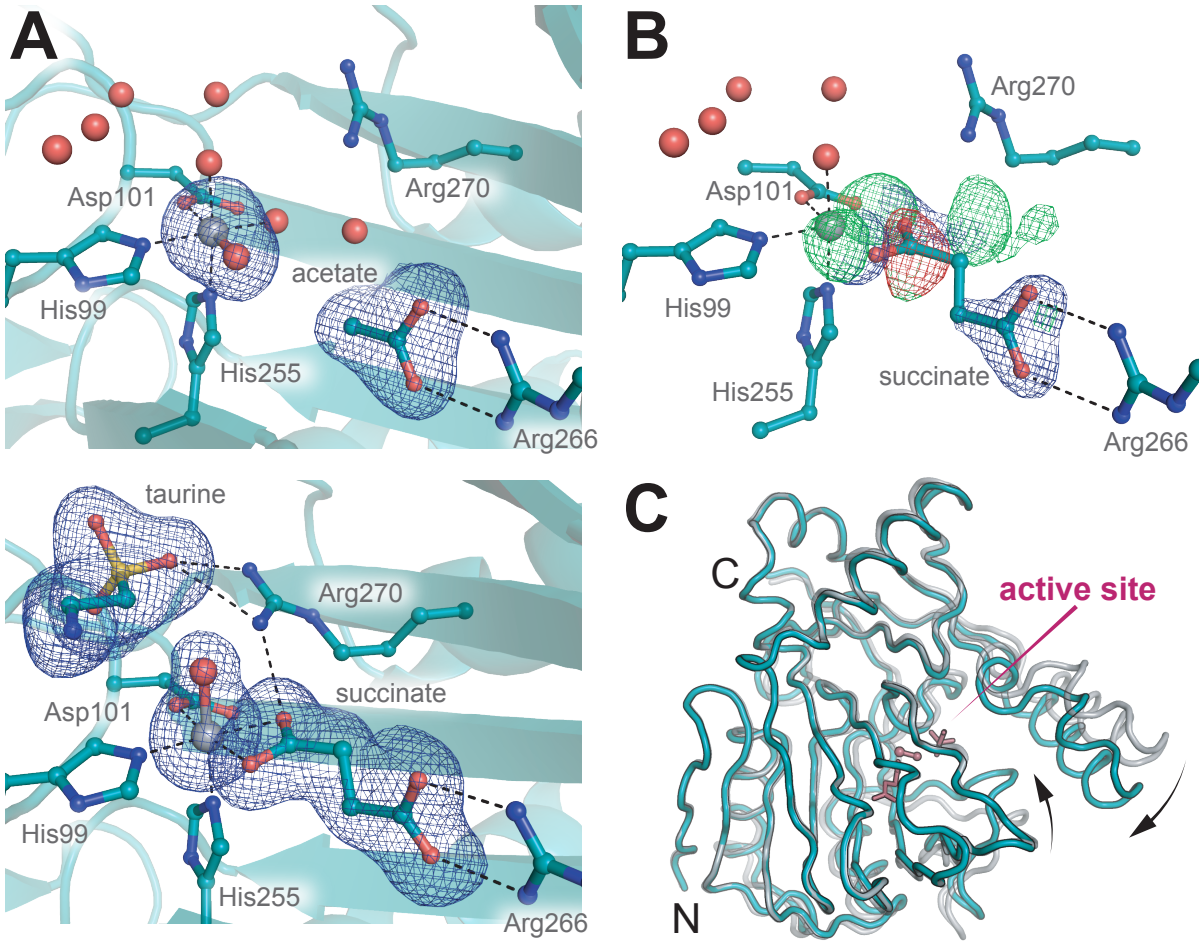

Figure S1. Comparison of chains A and B. (A) Polder omit maps[7] (blue mesh, contoured at 3.0σ) for cofactors and ligands present in chains A (*top*) and B (*bottom*). (B) Modeling of succinate into the chain A active site yields significant negative and positive difference density peaks indicative of a poor fit beyond the carboxylate interacting with Arg266. The $2F_o$-F_c (blue mesh) and F_o-F_c difference (green/red mesh) maps were contoured at 1.0σ and ±3.0σ around the ligand, respectively. (C) Alignment of chains A (grey) & B (turquoise) illustrates lid loop motion associated with substrate binding.

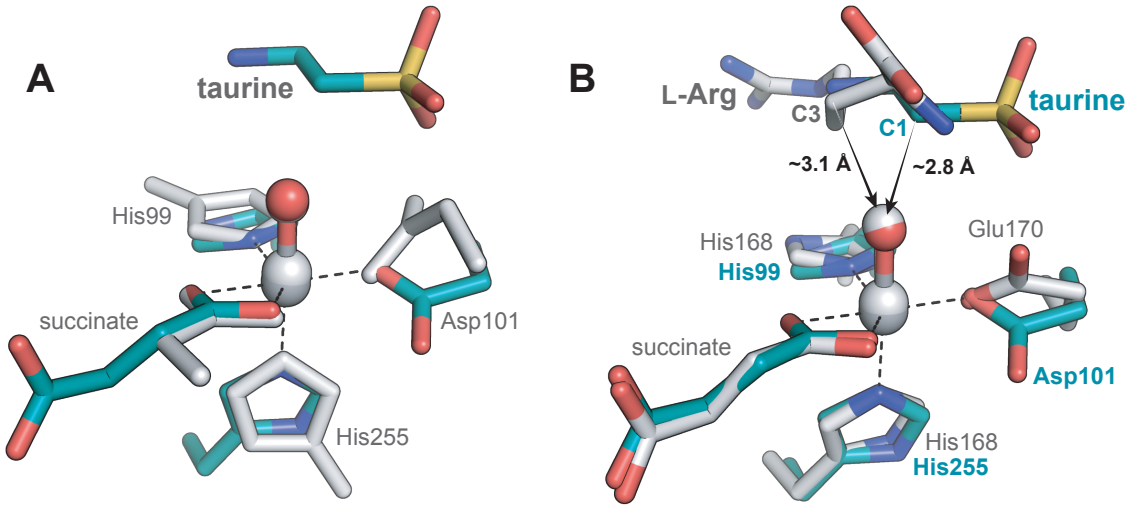

Figure S2. The first coordination sphere of vanadium aligns well with other models of the ferryl intermediate. Overlay of the TauD•vanadyl•taurine•succinate complex observed *in crystallo* with (A) a previously reported model of the TauD ferryl-oxo intermediate derived from DFT and Mössbauer studies[8] and (B) a structure of the VioC•vanadyl•taurine•succinate complex[9] (PDB accession code 6ALR). Structures were aligned using the coordinating atoms only, yielding an rmsd of 0.154 Å and 0.135 Å, respectively.

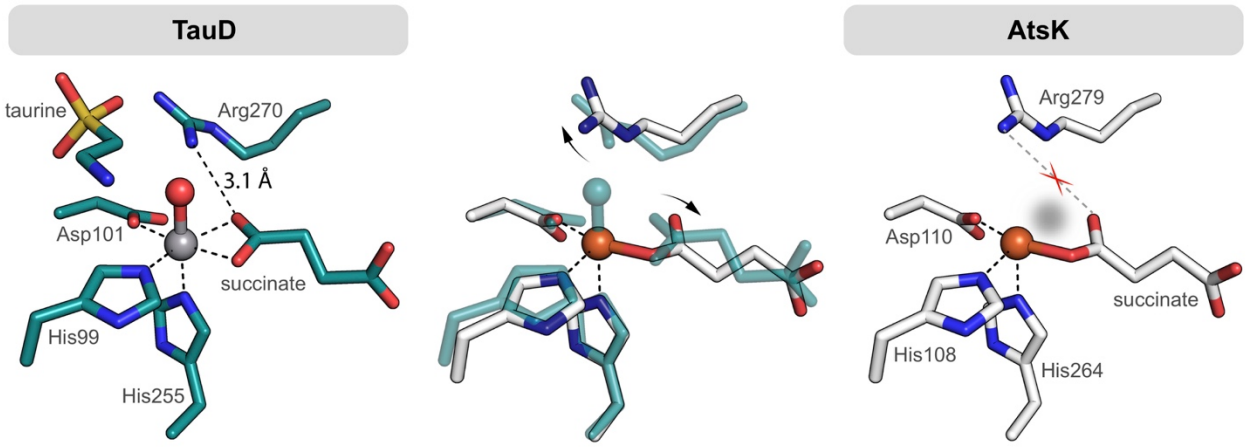

Figure S3. H-bonding interactions with an active site arginine influence the mode of succinate binding. In the absence of taurine, disorder in the Arg270 side chain may result in monodentate ligation of succinate, as observed in the AtsK•succinate structure[10] (PDB accession code 1VZ4), thereby enabling formation of an offline oxo species.

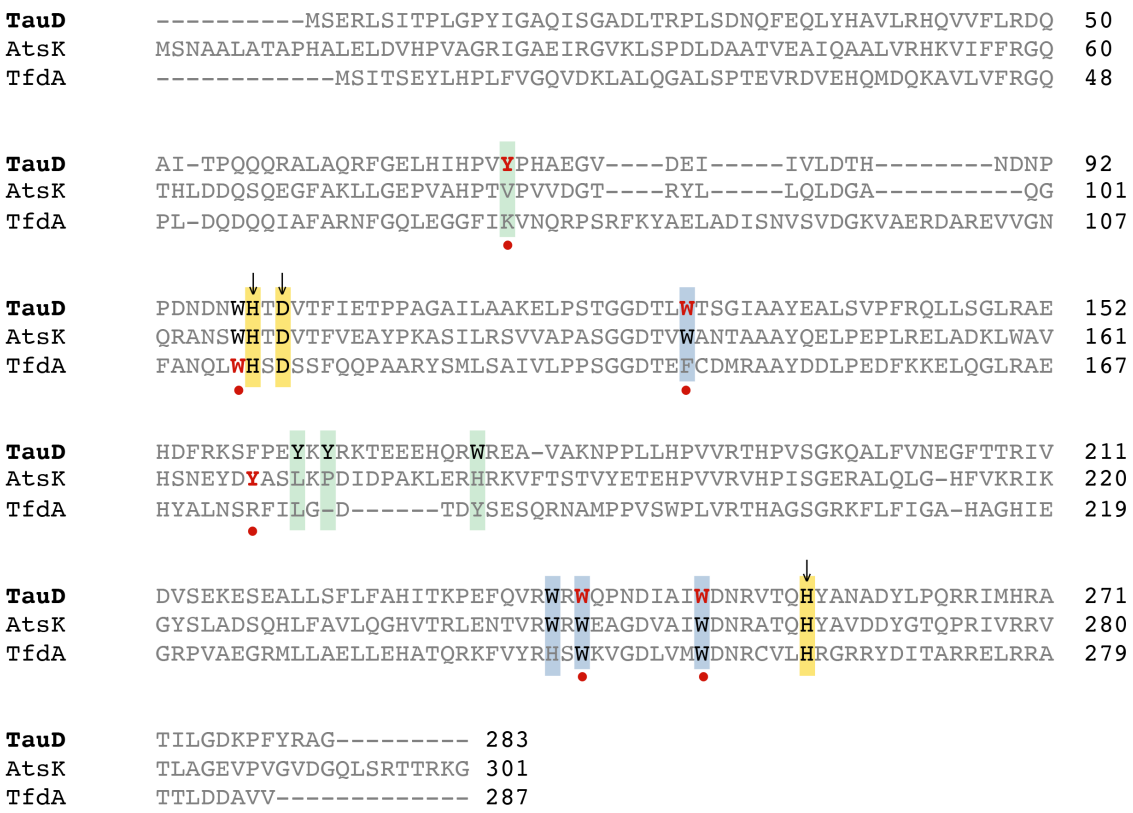

Figure S4. Sequence alignment of the related Fe/2OG hydroxylases TauD, AtsK and TfdA. Metal-coordinating residues are indicated in yellow and emphasized with arrows. Residues corresponding to the TauD tryptophan radical transfer pathway are highlighted in blue, while those associated with the tyrosine pathway are in green. Aromatic residues that have been experimentally observed hydroxylated or coordinated to the Fe center are bolded in red, and emphasized with red dots.[4, 10-12]

References

1. Price, J. C., Barr, E. W., Tirupati, B., Bollinger, J. M., Jr. and Krebs, C. (2003) The first direct characterization of a high-valent iron intermediate in the reaction of an α-ketoglutarate-dependent dioxygenase: A high-spin Fe(IV) complex in taurine/α-ketoglutarate dioxygenase (TauD) from *Escherichia coli*, *Biochemistry 42*, 7497-7508.
2. Otwinowski, Z., and Minor, W. (1997) Processing of x-ray diffraction data collected in oscillation mode, *Method. Enzymol. 276*, 307-326.
3. Long, F., Vagin, A. A., Young, P., and Murshudov, G. N. (2008) BALBES: A molecular-replacement pipeline, *Acta Crystallogr. D 64*, 125-132.
4. Elkins, J. M., Ryle, M. J., Clifton, I. J., Dunning Hotopp, J. C., Lloyd, J. S., Burzlaff, N. I., Baldwin, J. E., Hausinger, R. P., and Roach, P. L. (2002) X-ray crystal structure of *Escherichia coli* taurine/α-ketoglutarate dioxygenase complexed to ferrous iron and substrates, *Biochemistry 41*, 5185-5192.
5. Emsley, P., Lohkamp, B., Scott, W. G., and Cowtan, K. (2010) Features and development of Coot, *Acta Crystallogr. D 66*, 486-501.
6. Adams, P. D., Afonine, P. V., Bunkóczi, G., Chen, V. B., Davis, I. W., Echols, N., Headd, J. J., Hung, L.-W., Kapral, G. J., Grosse-Kunstleve, R. W., McCoy, A. J., Moriarty, N. W., Oeffner, R., Read, R. J., Richardson, D. C., Richardson, J. S., Terwilliger, T. C., and Zwart, P. H. (2010) PHENIX: A comprehensive python-based system for macromolecular structure solution, *Acta Crystallogr. D 66*, 213-221.
7. Liebschner, D., Afonine, P. V., Moriarty, N. W., Poon, B. K., Sobolev, O. V., Terwilliger, T. C., and Adams, P. D. (2017) Polder maps: Improving omit maps by excluding bulk solvent, *Acta Crystallogr. D 73*, 148-157.
8. Sinnecker, S., Svensen, N., Barr, E. W., Ye, S., Bollinger, J. M., Jr., Neese, F., and Krebs, C. (2007) Spectroscopic and computational evaluation of the structure of the high-spin Fe(IV)-oxo intermediates in taurine: α-ketoglutarate dioxygenase from *Escherichia coli* and its His99Ala ligand variant, *J. Am. Chem. Soc. 129*, 6168-6179.
9. Mitchell, A. J., Dunham, N. P., Martinie, R. J., Bergman, J. A., Pollock, C. J., Hu, K., Allen, B. D., Chang, W.-C., Silakov, A., Bollinger, J. M., Jr., Krebs, C., and Boal, A. K. (2017) Visualizing the reaction cycle in an iron(II)- and 2-(oxo)-glutarate-dependent hydroxylase, *J. Am. Chem. Soc. 139*, 13830-13836.
10. Müller, I., Stückl, C., Wakeley, J., Kertesz, M., and Usón, I. (2005) Succinate complex crystal structures of the α-ketoglutarate-dependent dioxygenase AtsK: Steric aspects of enzyme self-hydroxylation, *J. Biol. Chem. 280*, 5716-5723.
11. Liu, A., Ho, R. Y. N., Que, L., Jr., Ryle, M. J., Phinney, B. S., and Hausinger, R. P. (2001) Alternative reactivity of an α-ketoglutarate-dependent iron(II) oxygenase: Enzyme self-hydroxylation, *J. Am. Chem. Soc. 123*, 5126-5127.
12. Ryle, M. J., Liu, A., Muthukumaran, R. B., Ho, R. Y. N., Koehntop, K. D., McCracken, J., Que, L., Jr. and Hausinger, R. P. (2003) O_2- and α-ketoglutarate-dependent tyrosyl radical formation in TauD, an α-keto acid-dependent non-heme iron dioxygenase, *Biochemistry 42*, 1854-1862.